Cell Reports
Report

Acquired Resistance of EGFR-Mutant Lung Adenocarcinomas to Afatinib plus Cetuximab Is Associated with Activation of mTORC1

Valentina Pirazzoli,[1,12] Caroline Nebhan,[2,12] Xiaoling Song,[1] Anna Wurtz,[1] Zenta Walther,[3] Guoping Cai,[3] Zhongming Zhao,[2,4] Peilin Jia,[4] Elisa de Stanchina,[5] Erik M. Shapiro,[6] Molly Gale,[3] Ruonan Yin,[7] Leora Horn,[8] David P. Carbone,[9] Philip J. Stephens,[10] Vincent Miller,[10] Scott Gettinger,[1,11] William Pao,[2,8,13] and Katerina Politi[1,3,11,13,*]

[1]Yale Cancer Center, Yale University School of Medicine, New Haven, CT 06510, USA
[2]Department of Cancer Biology, Vanderbilt University School of Medicine, Nashville, TN 37232, USA
[3]Department of Pathology, Yale University School of Medicine, New Haven, CT 06510, USA
[4]Department of Biomedical Informatics, Vanderbilt University School of Medicine, Nashville, TN 37232, USA
[5]Antitumor Assessment Core, Molecular Pharmacology and Chemistry Program, Memorial Sloan-Kettering Cancer Center, New York, NY 10065, USA
[6]Department of Radiology, Michigan State University, East Lansing, MI 48824, USA
[7]Program in the Biological and Biomedical Science, Yale University School of Medicine, New Haven, CT 06510, USA
[8]Department of Medicine and Vanderbilt-Ingram Cancer Center, Vanderbilt University School of Medicine, Nashville, TN 37232, USA
[9]James Thoracic Center, The Ohio State University Medical Center, Columbus, OH 43210, USA
[10]Foundation Medicine Inc., Cambridge, MA 02141, USA
[11]Department of Medicine (Medical Oncology), Yale University School of Medicine, New Haven, CT 06510, USA
[12]Co-first author
[13]Co-senior author
*Correspondence: katerina.politi@yale.edu
http://dx.doi.org/10.1016/j.celrep.2014.04.014

SUMMARY

Patients with *EGFR*-mutant lung adenocarcinomas (LUADs) who initially respond to first-generation tyrosine kinase inhibitors (TKIs) develop resistance to these drugs. A combination of the irreversible TKI afatinib and the EGFR antibody cetuximab can be used to overcome resistance to first-generation TKIs; however, resistance to this drug combination eventually emerges. We identified activation of the mTORC1 signaling pathway as a mechanism of resistance to dual inhibition of EGFR in mouse models. The addition of rapamycin reversed resistance in vivo. Analysis of afatinib-plus-cetuximab-resistant biopsy specimens revealed the presence of genomic alterations in genes that modulate mTORC1 signaling, including *NF2* and *TSC1*. These findings pinpoint enhanced mTORC1 activation as a mechanism of resistance to afatinib plus cetuximab and identify genomic mechanisms that lead to activation of this pathway, revealing a potential therapeutic strategy for treating patients with resistance to these drugs.

INTRODUCTION

Targeted therapies effectively treat subsets of solid cancers. However, the inevitable development of acquired resistance (AR) has hampered their success. A paradigm for this concept is the case of epidermal growth factor receptor (*EGFR*)-mutant lung cancer. *EGFR* mutations (exon 19 deletions or the L858R point mutation) are associated with sensitivity to the first-generation tyrosine kinase inhibitors (TKIs) gefitinib and erlotinib (Pao and Chmielecki, 2010), but drug resistance emerges on average 1 year after TKI treatment. In ~50% of resistant tumors, the mutant *EGFR* allele has acquired a secondary mutation in exon 20 (T790M) (Pao and Chmielecki, 2010). Additional mechanisms of resistance include amplification of other receptor tyrosine kinases (RTKs) like *MET* and *HER2* (*ERBB2*), mutations in genes encoding downstream signaling components, or phenotypic transformations such as epithelial-to-mesenchymal transition (EMT) and neuroendocrine differentiation (Ohashi et al., 2013).

In a previous study using transgenic mice with $EGFR^{L858R+T790M}$-induced lung adenocarcinomas (LUADs), we showed that resistance due to EGFR T790M could be overcome using a combination of afatinib plus cetuximab (A+C) (Regales et al., 2009). Afatinib is a second-generation TKI that covalently binds EGFR at cysteine 797, while cetuximab is an anti-EGFR antibody. This preclinical study prompted a phase IB/II clinical trial testing this drug combination in patients with progressive disease after TKI treatment. The trial showed an overall 32% response rate with a median duration of response of 8 months (Janjigian et al., 2012). Unfortunately, patients responding to the drug combination still develop progressive disease.

We used xenografts and transgenic mice to model AR to the combination of A+C. Molecular analysis of resistant tumors revealed activation of the mTOR signaling pathway. Consistent with these findings, two separate patients with A+C-resistant tumors exhibited alterations in genes (*NF2* and *TSC1*) that when

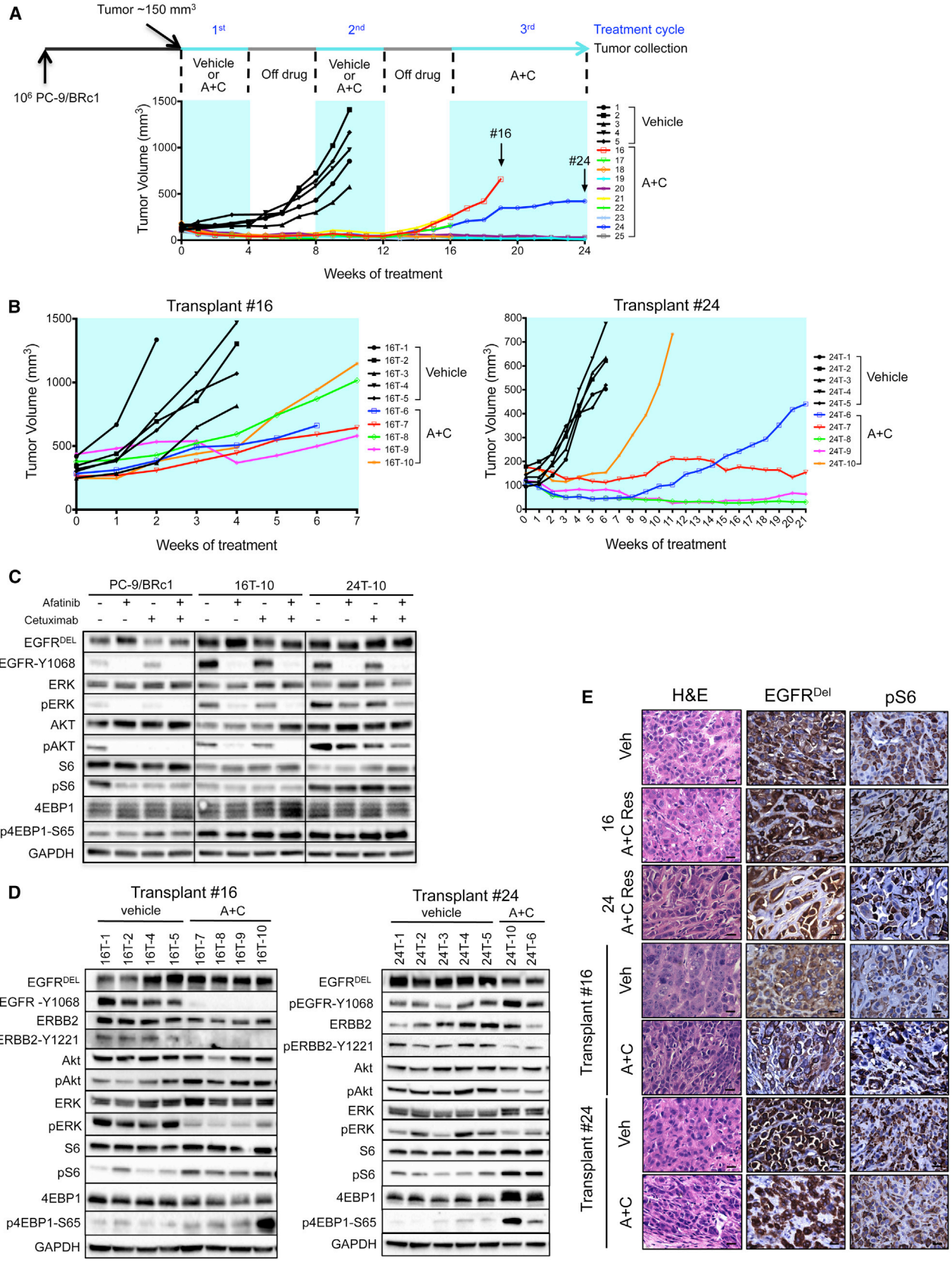

(legend on next page)

silenced in *EGFR*-mutant cells led to activation of the mTOR pathway. In vitro and in vivo, A+C resistance can be overcome by addition of an mTOR pathway inhibitor. These studies demonstrate mechanisms of AR to dual inhibition of EGFR in *EGFR*-mutant lung cancer and provide new insight into the biology of this subset of lung cancers, with immediate therapeutic implications for patients.

RESULTS

Acquired Resistance to A+C Combination Therapy in Xenografts

We previously modeled AR to erlotinib in tetracycline-inducible mouse models of EGFR-dependent lung cancer by intermittently treating mice with the TKI (Politi et al., 2010). We observed clinically relevant mechanisms of AR, such as the EGFR T790M mutation and *Met* amplification, validating this experimental approach. We adopted the same strategy to establish models of resistance to A+C, first in xenograft models using the PC-9/BRc1 human LUAD cell line that harbors an $EGFR^{\Delta E746\text{-}A750+T790M}$ mutation (Chmielecki et al., 2011). Immunocompromised mice with PC-9/BRc1-induced tumors were randomized to receive either vehicle (n = 5) or A+C (n = 10). After 1 month of treatment, drug administration was interrupted for 1 month, and this on/off drug treatment regimen was repeated three times (Figure 1A). All tumors in control mice grew continuously. In the A+C-treated cohort, tumors initially regressed. During the third cycle of treatment, two tumors (#16 and #24) became resistant (Figure 1A). These were reimplanted into mice and treated with A+C or vehicle alone for 4 weeks (Figure 1B). Eventually, we collected four A+C-resistant transplants from tumor #16 (labeled 16T-7, 16T-8, 16T-9, and 16T-10) and two from tumor #24 (24T-6 and 24T-10) (Table S1). Cell lines were established from tumors 16T-10 and 24T-10. Resistance to A+C in these cell lines compared to parental PC-9 and PC-9/BRc1 cells was confirmed in a 3D colony assay (Figure S1A).

Evidence for mTOR Pathway Activation in A+C-Resistant Xenografts

To identify mechanisms of resistance to A+C, we performed molecular analyses of the tumors collected. We first asked whether resistance to A+C could be explained by the acquisition of new mutations in *EGFR* or *ERBB2*, both of which are targets of A+C. Sequencing of control and A+C-resistant tumors did not detect any mutations in *EGFR* and *ERBB2* (data not shown). Analysis of the tumors revealed increased *EGFR* copy number in both vehicle-treated and A+C-resistant tumors compared to the parental PC-9/BRc1 cell line with tumor #16, but not #24, exhibiting high-level *EGFR* amplification (Figure S1B). Minor fluctuations in *ERBB2, MET*, and *IGF1R* copy number were also observed, the significance of which is likely limited given the magnitude of these changes. Together, the copy number data suggested that RTK amplification alone could not explain the resistance phenotype observed in our samples.

These results prompted us to further investigate RTK levels and pathway activation in A+C-resistant samples. The xenograft-derived cell lines exhibited higher levels of phospho (p)-EGFR, pERK, and pAKT compared to parental PC-9/BRc1 cells. However, the levels of activation of these proteins decreased in the presence of A+C, suggesting that the drugs retained the ability to block these pathways in A+C-resistant cells (Figure 1C). Interestingly, drug treatment did not affect the levels of pS6 or p4EBP1, markers of mTOR pathway activation, in the A+C-resistant lines in contrast to parental PC-9/BRc1 cells. This evidence suggests that pathway rewiring in resistant tumor cells leads to sustained activation of the mTORC1 pathway. Similarly, in vivo, the mTOR pathway was consistently engaged in all A+C-resistant xenografts, as measured by pS6 and p4EBP1 (Figures 1D and 1E). The levels of pAKT and pERK in the xenografts did not reveal a consistent pattern that would support either playing a major role in resistance to A+C in this model (Figure 1D). Together, these results suggest that while pAKT and pERK can be inhibited in A+C-resistant tumors, the tumors retain sustained activation of mTOR signaling that may play a role in resistance to A+C combination therapy. Whole-exome sequencing (WES) of the A+C-resistant #16 and #24 tumors did not detect mutations in 23 mTOR-pathway related genes, strongly suggesting that nonmutational processes account for sustained activation of this pathway in these tumors.

Highly Penetrant Resistance to A+C in Genetically Engineered Mouse Models of EGFR-Mutant Lung Cancer

In parallel, we developed models of resistance to A+C using transgenic mice with $EGFR^{L858R+T790M}$-induced LUADs. Tumors in these mice are resistant to erlotinib but sensitive to A+C (Regales et al., 2009). Thirty-eight *CCSP-rtTA*; *TetO-*$EGFR^{L858R+T790M}$

Figure 1. Activation of the mTOR Pathway in Afatinib plus Cetuximab-Resistant Xenografts

(A) Representation of the intermittent dosing protocol used to generate acquired resistance to afatinib and cetuximab in xenografts. Approximately 10^6 PC-9/BRc1 cells were injected subcutaneously into the flanks of immunocompromised mice. When tumors reached a volume of ~150 mm^3, mice were treated with vehicle (n = 5, in black) or A+C (n = 10, in color). After 1 month of treatment, drug administration was stopped for 1 month. The intermittent drug cycle was repeated three times. Tumor volume measurements are shown. Tumors indicated by the arrows (#16 and #24) acquired resistance to A+C.

(B) Tumor growth of the transplants derived from A+C-resistant tumors #16 (left) and #24 (right). The resistant tumors were further transplanted into ten nude mice and treated continuously with vehicle (in black, n = 5) or A+C (in color, n = 5). Transplants are labeled with the number of the original tumor they were derived from (#16 or 24), the letter "T," and a number.

(C) Immunoblotting analysis of extracts from PC-9/BRc1, 16T-10, and 24T-10 cells treated with afatinib (100 nM), cetuximab (10 μg/ml), or the A+C combination. Lysates were probed with the indicated antibodies; p, phospho.

(D) Immunoblotting analyses of tumor lysates from vehicle- and A+C-treated transplants derived from A+C-resistant tumors 16 and 24. Lysates were probed with the indicated antibodies; p, phospho.

(E) Hematoxylin and eosin staining (H&E) and IHC performed on paraffin sections of tumors derived from vehicle- and A+C-treated mice as indicated. Sections were stained with antibodies to EGFR exon 19 deletion mutant ($EGFR^{DEL}$) and phospho-S6 (pS6) as indicated. Original magnification ×40 is shown. Scale bars, 20 μm.

tumor-bearing mice were cycled on and off A+C using the protocol used for the xenograft experiments (Figure 2A). Tumor burden before and during treatment was tracked using magnetic resonance imaging at the beginning and end of each drug cycle. This on/off drug treatment schedule was repeated until lung tumors no longer responded to treatment and increased in size on magnetic resonance images (Figure 2A). All 38 mice that underwent the intermittent dosing treatment protocol developed resistance to the A+C combination. The majority of mice developed resistance after three cycles of A+C (21 out of 38); 15 mice developed resistance after two cycles and two mice after four cycles of drug treatment (Table S2A). The median tumor shrinkage during the first cycle of A+C was 80%, but this was attenuated during the second and third cycles of treatment (Figure 2B). Six mice that were treated without interruption with A+C also developed resistance to the drug combination (Figure S2A; Table S2B). Consistent with the emergence of resistance, tumors from the mice with AR displayed higher levels of proliferation and lower levels of apoptosis compared to tumors from mice that had undergone short-term A+C treatment (Figure S2B).

We explored whether A+C-resistant tumors showed any phenotypic differences compared to untreated tumors. *CCSP-rtTA*; *TetO-EGFR*$^{L858R+T790M}$ mice developed solid and papillary LUADs positive for the type II pneumocyte marker surfactant protein-C (SP-C) and for thyroid transcription factor-1 (TTF1) (Figure 2C). While most untreated adenocarcinomas were papillary, A+C-treated and resistant tumors almost invariably were solid and more poorly differentiated (Figure 2C).

Evidence for mTOR Pathway Activation in the A+C-Resistant Mouse LUADs

To elucidate further the pathways that may account for resistance to A+C, we sequenced the *EGFR* transgene and *Erbb2* from 23 resistant tumors. Similar to our observations in xenografts, we did not find mutations in these genes or in *Pik3ca, Pik3cb*, and *Kras* (n = 15; data not shown). A+C-resistant mouse LUADs did not show copy number alterations in the *EGFR* transgene or in endogenous *Egfr*, *Erbb2*, *Met*, and *Igf1r* (Figure S2C).

We then examined which signaling events might promote AR to A+C. As expected, we found that upon short-term (5 day) A+C treatment, phosphorylation of EGFR and Erbb2 was decreased. As a consequence, reduced levels of phosphorylated Erk were observed, but Akt phosphorylation did not change (Figure 2D). Phosphorylation of EGFR was greatly reduced or completely abrogated in all of the resistant tumors, and phosphorylation of Akt was consistently higher than in untreated tumors, suggesting the presence of compensatory mechanisms of activation of the PI3K pathway in these tumors. Similarly, phosphorylation of Erbb2 was not restored to untreated levels in the A+C-resistant tumors. Similar to the xenografts discussed previously, A+C-resistant tumors consistently showed increased pS6, suggesting that increased activation of mTORC1 may play a role in AR to A+C (Figures 2C and 2D).

Mutations in mTOR Signaling Pathway Genes Are Associated with Resistance to A+C in Human Tumors

Consistent with the preclinical modeling, we found genetic evidence for potential activation of the mTOR signaling pathway in tumor samples from two (of four analyzed) separate patients with AR to A+C (Figure 3; Table 1; see Supplemental Information for patient details). Strikingly, the mutated tumor genes were not shared between the two patients, but they both converged on the mTOR pathway. In the first patient, targeted resequencing of 182 genes using the FoundationOne platform (Table 1; Table S3) as well as WES revealed that the resected A+C-resistant tumor (Figures 3A and S3A) still harbored both the L858R and T790M mutations (frequencies of 0.38 of 1,162 reads and 0.24 of 1,279 reads, respectively, in the FoundationOne assay) (Jeselsohn et al., 2014). Unexpectedly, two additional mutations were found in *NF2* (c.592C>T_p.R198* at frequency 0.15 of 631 reads and c.811-2A>T: splice at 0.13 frequency of 1,168 reads). These two mutations were not detected in the 2006 tumor specimen, as assessed by amplicon-based deep resequencing (Table 1).

The *NF2* gene encodes Merlin, a protein with putative tumor-suppressive function. Both mutations are predicted to cause loss of protein function. The R198* mutation is a truncating mutation that causes loss of two-thirds of Merlin and has previously been described in cancers, including ependymoma (Lamszus et al., 2001). The c.811-2A>T alteration is a splice-site mutation that at a minimum affects the FERM domain, important for Merlin's localization and activation. In support of a functional role of this mutation, a 69 bp deletion encompassing this exon 9 splice site and causing *NF2* exon 9 skipping has been associated with familial autosomal dominant intramedullary ependymoma (Zemmoura et al., 2014).

In different cellular contexts, *NF2* has been shown in independent studies to negatively regulate EGFR signaling and mTORC1 (Curto et al., 2007; James et al., 2009; López-Lago et al., 2009). To determine whether the mTORC1 pathway was activated in this sample, we used immunohistochemistry (IHC) to stain the biopsy specimen collected at the time of resistance to A+C with a pS6 antibody and observed a strong signal (Figure 3B). In support of a role for *NF2* on TKI sensitivity, knockdown of *NF2* led to a decrease in the sensitivity of PC-9 cells to afatinib (Figure 3C). Importantly, the addition of an mTOR inhibitor, everolimus (RAD001), resensitized PC-9 cells with *NF2* knockdown to afatinib in vitro (Figure 3C). Notably, everolimus alone was not able to inhibit cell proliferation in cells treated with either control (scrambled) or *NF2* small interfering RNAs (siRNAs) (Figure S3C). The same effect was observed in HCC827 cells upon cetuximab treatment (Figure S3B). Moreover, A+C treatment in LUAD HCC827 cells did not decrease the levels of pS6 upon *NF2* knockdown (Figure S3B). Taken together, these patient and in vitro data suggest that the *NF2* mutations were acquired during treatment on A+C and that *NF2* loss leads to activation of the mTORC1 signaling pathway to mediate drug resistance.

In the second patient, initial molecular analysis of the A+C-resistant tumor (Figure 3D) did not detect the T790M mutation, *MET* amplification, or *ERBB2* amplification. Further analysis using a more recent FoundationOne panel (Frampton et al., 2013) revealed the presence of the L858R mutation (c.2573T>G; frequency of 0.19 of 715 reads) plus a mutation in the tuberous sclerosis 1 (*TSC1*) gene (c.345_345 delT_p.L116fs*; frequency 0.15 of 399 reads; this sample contained approximately 70% tumor cells) (Table 1; Table S3). The observed L116fs* frameshift mutation leads to the creation of a stop codon immediately

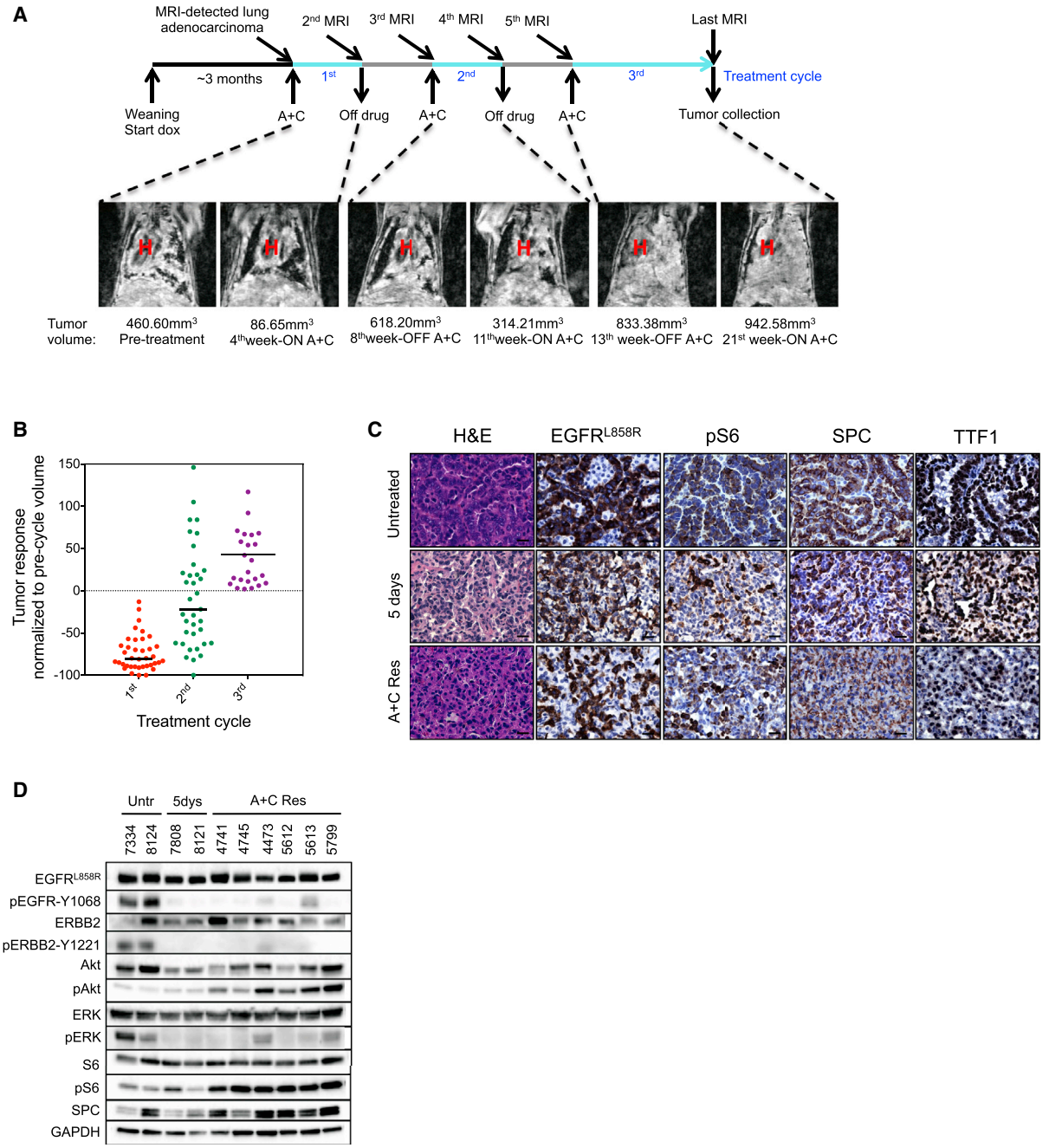

Figure 2. Activation of the mTOR Pathway in A+C-Resistant Mouse LUADs

(A) Intermittent dosing of A+C was performed on a 1-month-on and 1-month-off drug cycle. Doxycycline administration was initiated at weaning and subsequently kept constant throughout the life of the animal. Tumor response was evaluated by magnetic resonance imaging (MRI) at the beginning and at the end of every drug-treatment cycle. Coronal magnetic resonance images of a *CCSP-rtTA*; *TetO-EGFR*$^{L858R+T790M}$ mouse subjected to intermittent A+C treatment are shown. Tumor volume measurements are found below each image. H, heart.

(B) Tumor response in *CCSP-rtTA*; *TetO-EGFR*$^{L858R+T790M}$ mice subjected to the A+C intermittent treatment protocol. Tumor volume is plotted as the percentage of the tumor volume detected on the pre-cycle MRI. Median tumor volume change is −80% in the first cycle, −22% in the second cycle, and +29% at the third cycle of A+C.

(C) Hematoxylin and eosin staining (H&E) and IHC performed on paraffin sections of LUADs derived from *CCSP-rtTA*; *TetO-EGFR*$^{L858R+T790M}$ untreated mice and mice treated with A+C for 5 days or at resistance to the drug combination (A+C Res). Sections were stained with antibodies to EGFR^{L858R}, pS6, surfactant protein C (SPC), and thyroid transcription factor (TTF1) as indicated. Original magnification ×40 is shown. Scale bars, 20 μm.

(D) Immunoblotting analyses of tumor lysates from LUADs derived from untreated (Untr), A+C-treated (5 dys), or resistant (A+C res) *CCSP-rtTA*; *TetO-EGFR*$^{L858R+T790M}$ mice. Lysates were probed with the indicated antibodies; p, phospho.

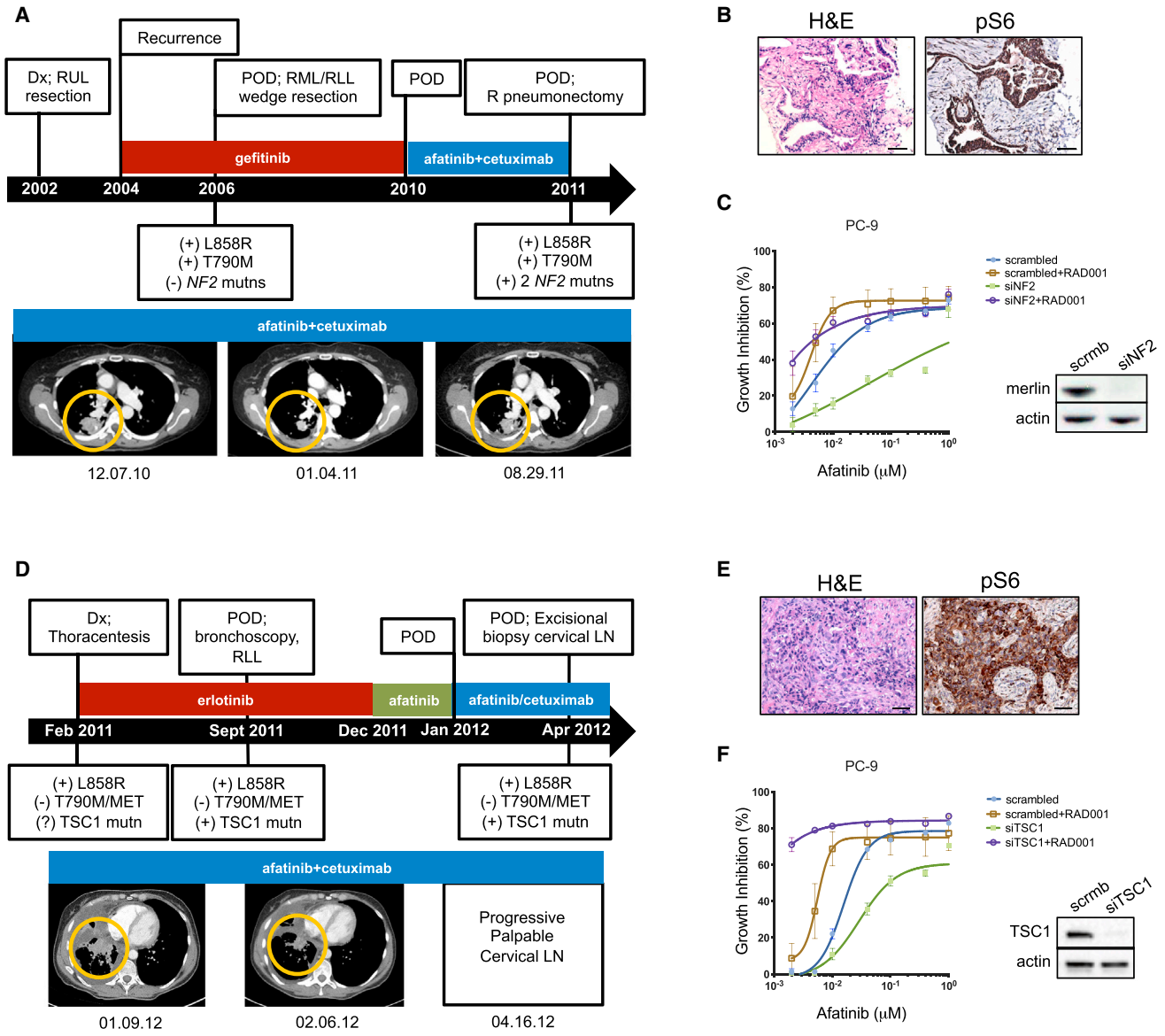

Figure 3. Genetic Alterations Associated with Activation of mTORC1 in Human Lung Tumors Resistant to A+C

(A) Top: disease milestones for patient 1. Time from diagnosis to A+C resistance is indicated by the black arrow. Clinical findings, procedures, and drug treatments are indicated above the arrow. Molecular findings are shown below the black arrow. Dx, diagnosis; POD, progression of disease; RUL, right upper lobe; RML, right middle lobe; RLL, right lower lobe; R, right; Mutns, mutations. Bottom: computed tomography scans of the lungs are shown prior to (12.07.10), during (01.04.11), and at resistance (08.29.11) to A+C. Tumors areas are circled.

(B) Hematoxylin and eosin (H&E; left) and IHC for pS6 (right) of the A+C-resistant tumor harboring the *NF2* mutations. Original magnification ×20 is shown. Scale bars, 50 μm.

(C) Growth inhibition of PC-9 cells after knockdown of *NF2* in response to afatinib (left). Viable cells were measured after 72 hr of treatment and plotted relative to untreated controls. Data are presented as the mean ± SE. Immunoblotting of PC-9 cells showing efficient knockdown of Merlin expression is shown on the right. Lysates were probed with the indicated antibodies. scrmb, scrambled siRNA.

(D) Top: disease milestones for patient 2. Time from diagnosis to A+C resistance is indicated by the black arrow. Clinical findings, procedures, and drug treatments are indicated above the arrow. Molecular findings are shown below the black arrow. Dx, diagnosis; POD, progression of disease; RLL, right lower lobe; Mutn, mutation; LN, lymph node. Bottom, computed tomography scans of the lungs are shown prior (01.09.12) and during treatment with A+C (02.06.12). Tumor areas are circled.

(E) H&E staining of the excised cervical lymph node from patient 2 (left) and IHC showing phosphorylation of S6 (pS6, right). Scale bars, 50 μm.

(F) Growth inhibition of PC-9 cells after knockdown of *TSC1* in response to afatinib (left). Viable cells were measured after 72 hr of treatment and plotted relative to untreated controls. Data are presented as the mean ± SE. Immunoblotting of PC-9 cells showing efficient knockdown of TSC1 expression is shown on the right. Lysates were probed with the indicated antibodies. scrmb, scrambled siRNA.

Table 1. List of Mutations Detected by Targeted Sequencing in Patient 1 and Patient 2

Gene	Nucleotide	Protein	Pre-A+C (Frequency, Total Reads)	Post-A+C (Frequency, Total Reads)
Patient 1				
EGFR	c.2573T>G	p.L858R	positive[a]	38%, 1,162
EGFR	c.2369C>T	p.T790M	positive[a]	24%, 1,279
NF2	c.592C>T	p.R198*	0%, 2,301	15%, 631
NF2	c.811-2A>T	splice	0%, 2,569	13%, 1,168
Patient 2				
EGFR	c.2573T>G	p.L858R	3%, 827	19%, 715
TSC1	c.345_345delT	p.L116fs*2	1%, 613	15%, 399

[a]As per a 2009 retrospective clinical report (Genzyme) of a 2006 biopsy sample.

downstream of codon 116, truncating the protein. The somatic status and zygosity of the *TSC1* L116fs*2 alteration (see Supplemental Experimental Procedures) were consistent with a somatic alteration clonally present on a single *TSC1* copy in the tumor, indicating that loss of heterozygosity (LOH) occurred. The *TSC1* mutation status of the pleural fluid collected at diagnosis was not assessed due to insufficient tumor material. FoundationOne analysis of the erlotinib-resistant lung specimen (before A+C) identified the presence of the *L858R* mutation (c.2573T>G; frequency of 0.03 of 827 reads) and of the *TSC1* mutation (c.345_345 delT_p.L116fs*; frequency 0.01 of 613 reads), indicating that it did preexist treatment with A+C (Table 1; Table S3). The low allele frequency of both of the mutations is due to low tumor purity of this sample (10% purity). These data suggest that selection of the deleterious *TSC1* mutant may have occurred during A+C treatment.

The *TSC1* gene encodes for Hamartin, which together with Tuberin (*TSC2*) forms a complex that suppresses mTORC1 signaling (Laplante and Sabatini, 2012). To determine whether this pathway was active in the sample collected after A+C treatment, we performed IHC for pS6 and observed strong staining (Figure 3E). The functional role of disruption of TSC1 on drug response was tested using siRNAs. Knockdown of *TSC1* in PC-9 cells led to a decrease in sensitivity of the cells to afatinib, and sensitivity to afatinib was restored by the addition of everolimus (Figure 3F). Moreover, cells treated with either scrambled or *TSC1* siRNAs were not sensitive to everolimus treatment (Figure S3C). These results indicate that the absence of *TSC1* mediates resistance to EGFR-directed therapies by activating the mTORC1 signaling pathway.

Xenografts and LUADs Resistant to A+C Are Sensitive to Concurrent EGFR and mTOR Inhibition

Activation of the mTOR pathway in mouse models and patient samples led us to explore whether A+C-resistant tumors responded to inhibition of this pathway. To test this, we treated four *CCSP-rtTA*; *TetO-EGFR*$^{L858R+T790M}$ mice with A+C-resistant tumors with rapamycin as a single agent. Rapamycin treatment alone was ineffective in all four cases (Figures 4A and 4C). This result is in line with previous findings showing that inhibition of mTOR alone is not sufficient to abolish Akt signaling and that the combination of an mTOR inhibitor with an RTK inhibitor is more likely to have antitumor activity (Li et al., 2008; Rodrik-Outmezguine et al., 2011). To test whether combined inhibition of EGFR and mTOR could overcome resistance to A+C, we added rapamycin to the treatment regimen of *CCSP-rtTA*; *TetO-EGFR*$^{L858R+T790M}$ mice at the time of emergence of resistance to afatinib plus cetuximab (A+C+R). All eight mice with LUADs resistant to A+C responded dramatically to the addition of rapamycin (Figures 4B and 4C). In the mice with tumor burden lower than 600 mm^3 (six out of eight), tumor shrinkage was greater than 72% after 1 month of treatment with A+C+R (Figure 4B; Table S4). We also stained paraffin-embedded sections of A+C-resistant LUADs treated with rapamycin alone or in combination with A+C with antibodies against phosphohistone H3 and cleaved caspase-3 (Figure S4). Tumors treated with rapamycin alone were not growth inhibited, while tumors treated with A+C+R exhibited both proliferation arrest and cell death. We further found that addition of rapamycin to A+C decreased pS6 in the LUADs (Figure 4D). All four of the A+C-resistant tumors treated with rapamycin alone showed activation of EGFR and Erbb2, as expected by the absence of EGFR-directed therapies (Figure 4D).

To evaluate the effect of concurrent EGFR and mTOR inhibition in xenografts, we injected 10^6 cells derived from the A+C-resistant xenografts 16T-10 and 24T-10 into immunodeficient mice. Upon the growth of A+C-resistant tumors, mice were divided into three groups (Figure 4E). One group was maintained on A+C for 4 weeks (n = 7). The second group was treated with rapamycin alone (R; n = 2), and the third group was treated with rapamycin in addition to A+C (A+C+R; n = 5). Tumors in the A+C combination and rapamycin arms grew throughout the 4 weeks. In contrast, all of the tumors in mice that received A+C+R shrank (Figure 4F). Together, these data indicate that inhibition of mTORC1 can resensitize cells to A+C treatment.

DISCUSSION

We show that resistance to dual inhibition of *EGFR*$^{L858R+T790M}$ with A+C is due to activation of mTORC1 signaling in mouse models. Addition of drugs targeting mTOR resensitizes tumors to A+C treatment. Consistent with these findings, we have identified mutations in genes that affect the mTOR signaling cascade in A+C-resistant biopsy samples from two separate patients with *EGFR* mutant lung cancer.

Previous studies have shown that the presence of active mTORC1 in untreated *EGFR*-mutant tumors is a direct consequence of mutant EGFR signaling. Effective therapies that target mutant EGFR lead to a decrease in mTORC1 signaling and consequent tumor regression. Indeed, in cell lines harboring EGFR TKI-sensitizing mutations (e.g., *EGFR*^{L858R}), EGFR blockade using TKIs leads to a decrease in pS6 equivalent to that observed with rapamycin, accompanied by a decrease in cell viability (Li et al., 2007). Further supporting the critical role of mTORC1 signaling in the maintenance of *EGFR*-mutant lung tumors, the combination of either afatinib or HKI-272 with rapamycin together was required to elicit regression of *EGFR*$^{L858R+T790M}$-induced tumors (Li et al., 2007, 2008). Our study shows that in addition to playing a role in the maintenance

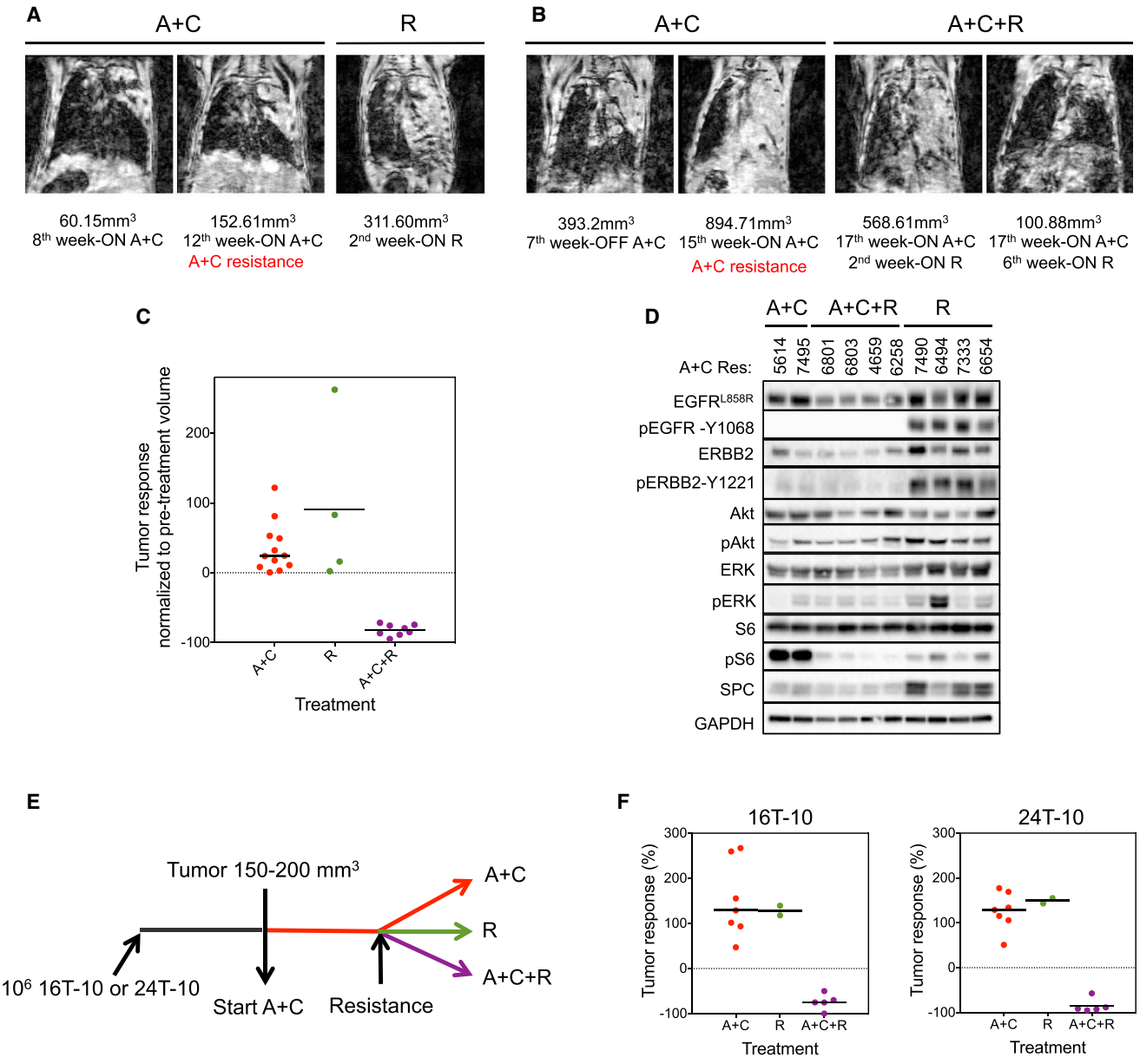

Figure 4. Tumors Resistant to A+C Are Sensitive to Concurrent EGFR and mTOR Inhibition

(A) Coronal MR images of *CCSP-rtTA*; *TetO-EGFR*$^{L858R+T790M}$ mouse lungs prior to and upon treatment with rapamycin (R) following the development of resistance to A+C as indicated in red. Tumor volume measurements are shown.

(B) Coronal magnetic resonance images of *CCSP-rtTA*; *TetO-EGFR*$^{L858R+T790M}$ mouse lungs prior to and upon treatment with rapamycin in combination with afatinib and cetuximab (A+C+R) following the development of resistance to A+C as indicated in red. Tumor volume measurements are shown.

(C) Response of A+C-resistant LUADs from *CCSP-rtTA*; *TetO-EGFR*$^{L858R+T790M}$ mice to 4 weeks of treatment with rapamycin alone (R) or in combination with afatinib and cetuximab (A+C+R). The increase in tumor volume in the presence of A+C before the randomization to R or A+C+R is shown on the left. Tumor volumes are plotted as the percentage of the tumor volume detected in the precycle magnetic resonance imaging. Median tumor volume change to R is +52% and to A+C+R is −79%.

(D) Immunoblotting analysis of LUADs resistant to A+C, following 4 weeks of treatment with rapamycin alone or in combination with afatinib and cetuximab. Lysates were probed with the indicated antibodies; p, phospho.

(E) Strategy used to test the response of A+C-resistant xenograft tumors to concurrent EGFR and mTOR inhibition. Approximately 10^6 16T-10 or 24T-10 cells were injected subcutaneously into immunocompromised mice. When tumors reached a volume between 150 and 200 mm^3, mice were treated with A+C (n = 14). When resistance emerged, two mice were switched to rapamycin treatment (R, 2 mg/kg per day) and five mice received A+C+R. The rest of the mice were maintained on A+C. Mice were treated for 4 weeks from the randomization point.

(F) Tumor response to A+C, rapamycin alone (R), or in combination (A+C+R) in xenografts. Data are plotted as percentage of tumor volume change from the randomization point. The median response to A+C+R was −75% in xenografts derived from 16T-10 cells (left) and −91% in xenografts derived from 24T-10 cells (right).

of *EGFR*-mutant lung tumors, the mTORC1 pathway also plays a role in resistance to EGFR-directed therapies, specifically following A+C treatment. First, pS6 is observed in cell lines, xenografts, and genetically engineered mouse models of A+C-resistant *EGFR*-mutant lung cancer. Second, these tumors regress following the addition of rapamycin to A+C. These data highlight the importance of mTORC1 for the survival of lung cancer cells with *EGFR* mutations and suggest that as resistance emerges, tumors increasingly rely on mTORC1 activation to survive.

The presence of a *TSC1* frameshift mutation coupled with LOH at the same locus in a sample from a patient biopsied upon progression with A+C provides further evidence for dysregulation of the mTOR pathway as a mechanism of resistance to A+C. Indeed, strong pS6 staining was observed in tumor cells in this sample, and disruption of *TSC1* in human *EGFR*-mutant lung cancer cell lines increased their viability in the presence of EGFR TKIs. Unexpectedly, acquired *NF2* inactivating mutations were observed in A+C-resistant specimens from a separate patient on the same trial. Recent work has found that a downstream biochemical consequence of *NF2* loss is activation mTORC1 (López-Lago et al., 2009). We show that the effects of both *TSC1* and *NF2* loss can be reversed in cells by treatment with a rapalog, suggesting that the presence of genomic changes in these genes indicates sensitivity to mTOR inhibition. Further studies to determine the prevalence of *NF2* and *TSC1* mutations in *EGFR*-mutant lung cancer are ongoing.

mTORC1 represents the output of several signaling pathways and external stimuli. In addition to genetic mechanisms like those described above that lead to its activation, it can be engaged through nongenetic mechanisms. Increased growth factor receptor signaling, through, for example, IGF1R, activates mTORC1 through the PI3K pathway. In this setting, one would expect to observe higher levels of phosphorylation of mTORC1 and AKT. Consistent with the possibility of similar mechanisms occurring in some of our models, we observed increased phosphorylation of AKT in the #16 xenograft-derived tumors and in the A+C-resistant genetically engineered mouse model tumors (Figures 1D and 2D). An increase in the levels of phosphorylation of IGF1R was indeed observed in the #16-derived tumors (data not shown) and may explain the increased mTORC1 signaling found in these tumors. These results also highlight how activation of mTORC1 can occur both via signals upstream and downstream of AKT. Moreover, our data from cell lines, xenografts, and patient samples suggest that mTORC1 activation acts cell autonomously in the tumor cells to confer resistance. Whether this pathway is also activated in other cells in the tumor microenvironment cannot be excluded and is under further investigation.

Our findings suggest that patients with AR to A+C may benefit from drug combinations that include EGFR-directed therapies and mTOR inhibitors. In this regard, a phase IB trial of afatinib with the rapalog sirolimus in patients with *EGFR*-mutant lung cancer is currently ongoing. Phase III trials of A+C in patients with TKI-naive and refractory *EGFR*-mutant lung cancer are planned. Inhibition of mTOR in this context may delay resistance. Due to concerns about the toxicity of this multidrug combination, it will be important to use preclinical models to determine whether continuous or intermittent dosing of the mTOR inhibitor are equally effective at countering drug resistance. Moreover, rapalogs only partially block downstream functions of mTOR in contrast to mTORC1/2 kinase inhibitors. Investigation of these latter novel agents will be informative to determine their efficacy in the context of *EGFR*-mutant lung cancer. Finally, the recent development of mutant-specific EGFR inhibitors that induce reduced toxicity due to less inhibition of wild-type EGFR may open the door to the use of drug combinations including those of EGFR inhibitors with mTOR inhibitors (Walter et al., 2013).

In summary, resistance to targeted therapies remains the major hurdle to the long-term success of EGFR-directed therapies. Our data in multiple preclinical models and human tumor samples show increased mTORC1 signaling after long-term treatment with A+C, identifying this node as a critical vulnerability of drug-resistant cells.

EXPERIMENTAL PROCEDURES

Transgenic Mice and Xenografts

All animals were kept in pathogen-free housing under guidelines approved by the Memorial Sloan Kettering Cancer Center (MSKCC) and Yale institutional animal care and use committees. *TetO-EGFR*$^{L858R+T790M}$ mice (Regales et al., 2007) and *CCSP-rtTA* mice were previously described (Tichelaar et al., 2000). For xenografts, 8-week-old nu/nu athymic nude mice (Harlan Labs) were injected subcutaneously with 10×10^6 PC-9/BRc1 cells together with Matrigel (BD Biosciences). Mice were randomized to receive either drug diluent alone (vehicle) or A+C. Tumor size was measured twice a week using calipers. To further propagate A+C-resistant tumors, these were minced and immediately injected subcutaneously with Matrigel (tumor #16) or cultured for 2 weeks then reinjected subcutaneously into immunodeficient mice (tumor #24). Afatinib (produced by the Organic Synthesis Core Facility at MSKCC) was suspended in 0.5% (w/v) methylcellulose and administered orally (25 mg/kg per day 5 days a week). Cetuximab (Erbitux; Bristol-Myers Squibb and Eli Lilly Pharmaceuticals) was purchased and administered intraperitoneally (1 mg twice a week). Rapamycin (LC Laboratories) was suspended in 0.5% carboxymethylcellulose and given orally at 2 mg/kg per day 5 days a week.

Cell Culture

Human LUAD cell lines PC-9, PC-9/BRc1, and HCC827 were used (Chmielecki et al., 2011). A+C-resistant cells, obtained from xenograft tumors, were kept in culture in presence of afatinib (250 nM) and cetuximab (10 μg/ml).

Immunoblotting

Cells and crushed tumors were lysed in ice-cold RIPA lysis buffer (50 mM Tris [pH 8.0], 150 mM NaCl, 5 mM MgCl, 1% Triton X-100, 0.5% sodium deoxycholate, 0.1% SDS, and protease and phosphatase inhibitor cocktail; Thermo Scientific). For cell-treatment studies, cells were starved overnight, treated with drugs for 8 hours, and washed twice with cold PBS before lysate preparation. Equal amounts of total protein were separated by SDS-PAGE and probed as indicated. Signals were detected using either SuperSignal West Pico or Femto chemiluminescent substrates (Pierce Biotechnology). For a list of antibodies, see Supplemental Experimental Procedures.

ACCESSION NUMBERS

The NCBI Sequence Read Archive (http://www.ncbi.nlm.nih.gov/sra) accession number for new data reported in this paper is SRP040807.

SUPPLEMENTAL INFORMATION

Supplemental Information includes Supplemental Experimental Procedures, four figures, and four tables and can be found with this article online at http://dx.doi.org/10.1016/j.celrep.2014.04.014.

AUTHOR CONTRIBUTIONS

V.P. and C.N. designed the study, performed experiments, analyzed the data, and wrote the manuscript. X.S., E.d.S., Z.Z., P.J., M.G., E.S., and R.Y. performed experiments and analyzed data. A.W., Z.W., G.C., L.H., D.C., P.S., V.M., and S.G. contributed to the analysis of patient samples. W.P. and K.P. supervised and designed the study and wrote the manuscript.

ACKNOWLEDGMENTS

The authors acknowledge support from the NIH/National Cancer Institute grants R00-CA131488 (K.P.), R01-CA120247 (K.P.), R01-CA121210 (W.P. and K.P.), P01-CA129243 (W.P. and M. Kris PI), U54-CA143798 (W.P. and F. Michor PI), F30-CA180353 (C.N.), DP2OD004362 (E.M.S.) and P30 CA008748 (E.d.S.). This work was also supported by the American Italian Cancer Foundation (V.P.), Uniting Against Lung Cancer (K.P. and X.S.), the VICC Cancer Center Core grant P30-CA68485 (W.P. and J. Pietenpol PI), VICC Melly Family Scholarship (C.N.), and the Ingram Professorship (Z.Z.). P.J.S. and V.M. are both employees and stockholders of Foundation Medicine Inc. A patent relating to EGFR T790M mutation testing was licensed on behalf of W.P., K.P., V.M., and others by Memorial Sloan-Kettering Cancer Center to MolecularMD. We thank the Yale Magnetic Resonance Research Center for assistance with MRIs.

Received: December 25, 2013
Revised: March 2, 2014
Accepted: April 8, 2014
Published: May 8, 2014

REFERENCES

Chmielecki, J., Foo, J., Oxnard, G.R., Hutchinson, K., Ohashi, K., Somwar, R., Wang, L., Amato, K.R., Arcila, M., Sos, M.L., et al. (2011). Optimization of dosing for EGFR-mutant non-small cell lung cancer with evolutionary cancer modeling. Sci. Transl. Med. *3*, 90ra59.

Curto, M., Cole, B.K., Lallemand, D., Liu, C.H., and McClatchey, A.I. (2007). Contact-dependent inhibition of EGFR signaling by Nf2/Merlin. J. Cell Biol. *177*, 893–903.

Frampton, G.M., Fichtenholtz, A., Otto, G.A., Wang, K., Downing, S.R., He, J., Schnall-Levin, M., White, J., Sanford, E.M., An, P., et al. (2013). Development and validation of a clinical cancer genomic profiling test based on massively parallel DNA sequencing. Nat. Biotechnol. *31*, 1023–1031.

James, M.F., Han, S., Polizzano, C., Plotkin, S.R., Manning, B.D., Stemmer-Rachamimov, A.O., Gusella, J.F., and Ramesh, V. (2009). NF2/merlin is a novel negative regulator of mTOR complex 1, and activation of mTORC1 is associated with meningioma and schwannoma growth. Mol. Cell. Biol. *29*, 4250–4261.

Janjigian, Y.Y., Smit, E.F., Horn, L., Groen, H.J.M., Camidge, D.R., Gettinger, S., Fu, Y., Denis, L.J., Miller, V., and Pao, W. (2012). Activity of afatinib/cetuximab in patients with EGFR mutant non-small cell lung cancer and acquired resistance to EGFR inhibitors. Ann. Oncol. *23*, ix400–ix446.

Jeselsohn, R., Yelensky, R., Buchwalter, G., Frampton, G.M., Meric-Bernstam, F., Gonzalez-Angulo, A.M., Ferrer-Lozano, J., Perez-Fidalgo, J.A., Cristofanilli, M., Gómez, H., et al. (2014). Emergence of constitutively active estrogen receptor-alpha mutations in pretreated advanced estrogen receptor positive breast cancer. Clin. Cancer Res. *20*, 1757–1767.

Lamszus, K., Lachenmayer, L., Heinemann, U., Kluwe, L., Finckh, U., Höppner, W., Stavrou, D., Fillbrandt, R., and Westphal, M. (2001). Molecular genetic alterations on chromosomes 11 and 22 in ependymomas. Int. J. Cancer *91*, 803–808.

Laplante, M., and Sabatini, D.M. (2012). mTOR signaling. Cold Spring Harb. Perspect. Biol. *4*, 4.

Li, D., Shimamura, T., Ji, H., Chen, L., Haringsma, H.J., McNamara, K., Liang, M.C., Perera, S.A., Zaghlul, S., Borgman, C.L., et al. (2007). Bronchial and peripheral murine lung carcinomas induced by T790M-L858R mutant EGFR respond to HKI-272 and rapamycin combination therapy. Cancer Cell *12*, 81–93.

Li, D., Ambrogio, L., Shimamura, T., Kubo, S., Takahashi, M., Chirieac, L.R., Padera, R.F., Shapiro, G.I., Baum, A., Himmelsbach, F., et al. (2008). BIBW2992, an irreversible EGFR/HER2 inhibitor highly effective in preclinical lung cancer models. Oncogene *27*, 4702–4711.

López-Lago, M.A., Okada, T., Murillo, M.M., Socci, N., and Giancotti, F.G. (2009). Loss of the tumor suppressor gene NF2, encoding merlin, constitutively activates integrin-dependent mTORC1 signaling. Mol. Cell. Biol. *29*, 4235–4249.

Ohashi, K., Maruvka, Y.E., Michor, F., and Pao, W. (2013). Epidermal growth factor receptor tyrosine kinase inhibitor-resistant disease. J. Clin. Oncol. *31*, 1070–1080.

Pao, W., and Chmielecki, J. (2010). Rational, biologically based treatment of EGFR-mutant non-small-cell lung cancer. Nat. Rev. Cancer *10*, 760–774.

Politi, K., Fan, P.D., Shen, R., Zakowski, M., and Varmus, H. (2010). Erlotinib resistance in mouse models of epidermal growth factor receptor-induced lung adenocarcinoma. Dis. Model. Mech. *3*, 111–119.

Regales, L., Balak, M.N., Gong, Y., Politi, K., Sawai, A., Le, C., Koutcher, J.A., Solit, D.B., Rosen, N., Zakowski, M.F., and Pao, W. (2007). Development of new mouse lung tumor models expressing EGFR T790M mutants associated with clinical resistance to kinase inhibitors. PLoS ONE *2*, e810.

Regales, L., Gong, Y., Shen, R., de Stanchina, E., Vivanco, I., Goel, A., Koutcher, J.A., Spassova, M., Ouerfelli, O., Mellinghoff, I.K., et al. (2009). Dual targeting of EGFR can overcome a major drug resistance mutation in mouse models of EGFR mutant lung cancer. J. Clin. Invest. *119*, 3000–3010.

Rodrik-Outmezguine, V.S., Chandarlapaty, S., Pagano, N.C., Poulikakos, P.I., Scaltriti, M., Moskatel, E., Baselga, J., Guichard, S., and Rosen, N. (2011). mTOR kinase inhibition causes feedback-dependent biphasic regulation of AKT signaling. Cancer Discov. *1*, 248–259.

Tichelaar, J.W., Lu, W., and Whitsett, J.A. (2000). Conditional expression of fibroblast growth factor-7 in the developing and mature lung. J. Biol. Chem. *275*, 11858–11864.

Walter, A.O., Sjin, R.T., Haringsma, H.J., Ohashi, K., Sun, J., Lee, K., Dubrovskiy, A., Labenski, M., Zhu, Z., Wang, Z., et al. (2013). Discovery of a mutant-selective covalent inhibitor of EGFR that overcomes T790M-mediated resistance in NSCLC. Cancer Discov. *3*, 1404–1415.

Zemmoura, I., Vourc'h, P., Paubel, A., Parfait, B., Cohen, J., Bilan, F., Kitzis, A., Rousselot, C., Parker, F., François, P., and Andres, C.R. (2014). A deletion causing NF2 exon 9 skipping is associated with familial autosomal dominant intramedullary ependymoma. Neuro-oncol. *16*, 250–255.